Hindawi
Wireless Communications and Mobile Computing
Volume 2023, Article ID 9824989, 1 page
https://doi.org/10.1155/2023/9824989

*Retraction*

# Retracted: Fast Target Detection Algorithm Based on CFAR and Target Variance Characteristics

**Wireless Communications and Mobile Computing**

Received 17 October 2023; Accepted 17 October 2023; Published 18 October 2023



This article has been retracted by Hindawi following an investigation undertaken by the publisher [1]. This investigation has uncovered evidence of one or more of the following indicators of systematic manipulation of the publication process:

(1) Discrepancies in scope
(2) Discrepancies in the description of the research reported
(3) Discrepancies between the availability of data and the research described
(4) Inappropriate citations
(5) Incoherent, meaningless and/or irrelevant content included in the article
(6) Peer-review manipulation

The presence of these indicators undermines our confidence in the integrity of the article's content and we cannot, therefore, vouch for its reliability. Please note that this notice is intended solely to alert readers that the content of this article is unreliable. We have not investigated whether authors were aware of or involved in the systematic manipulation of the publication process.

Wiley and Hindawi regrets that the usual quality checks did not identify these issues before publication and have since put additional measures in place to safeguard research integrity.

We wish to credit our own Research Integrity and Research Publishing teams and anonymous and named external researchers and research integrity experts for contributing to this investigation.

The corresponding author, as the representative of all authors, has been given the opportunity to register their agreement or disagreement to this retraction. We have kept a record of any response received.

## References

[1] L. Zhang, D. Sun, L. Wang, Z. Wang, and J. Wang, "Fast Target Detection Algorithm Based on CFAR and Target Variance Characteristics," *Wireless Communications and Mobile Computing*, vol. 2022, Article ID 5878443, 9 pages, 2022.

Hindawi
Wireless Communications and Mobile Computing
Volume 2022, Article ID 5878443, 9 pages
https://doi.org/10.1155/2022/5878443

*Research Article*

# Fast Target Detection Algorithm Based on CFAR and Target Variance Characteristics

**Lijuan Zhang,[1,2] Donglai Sun,[1,2] Lu Wang,[1] Zhengbo Wang,[1] and Jianqiang Wang[1]**

[1]*Department of Electrical Automation, Hebei University of Water Resources and Electric Engineering, Cangzhou, 061001 Hebei, China*
[2]*Water Resources Automation and Informatization Application Technology Research and Development Center of Hebei Colleges, Cangzhou, 061001 Hebei, China*

Correspondence should be addressed to Donglai Sun; sundonglai@hbwe.edu.cn

Received 7 March 2022; Revised 12 May 2022; Accepted 17 May 2022; Published 6 June 2022

Academic Editor: Rashid A Saeed



Target detection is a complex process that is important as an important module in computer vision applications. In particular, in many occasions where the real-time requirements are extremely high, it is very important to achieve fast and accurate detection of targets. But at this stage, there are still many problems in the research on rapid target detection, such as inefficiency and high is the first phase of automatic target recognition (ATR). For the performance of SAR image target detection, this paper proposes a CFAR fast detection algorithm based on Rayleigh. CFAR detection is divided into two steps: horizontal and vertical CFAR detection. The efficiency of parameter estimation is improved by the coincidence of adjacent point reference windows and the distribution characteristics of images. The algorithm in this paper combines the target variance characteristics to reduce the false alarm rate. The experiment was performed on the MSTAR dataset. Fast target detection algorithm based on CFAR and target variance feature has the characteristics of high detection rate, low false alarm, and high speed, and its detection performance is good. The experimental results show that the recognition efficiency of the proposed algorithm is higher than that of the traditional algorithm on different target datasets, the time is shortened by 30%, and the accuracy rate is equal to that of the traditional algorithm.



## 1. Introduction

Target detection is automatically detecting the target existing in the image, determining the semantic category of the target object and its specific location. That is to say, target detection is a complex process that not only needs to distinguish objects but also uses a bounding box to circle its specific position in the image from the background. As a very important module in computer vision applications, target detection has always been one of the core issues in the field of computer vision in many occasions where real-time requirements are extremely high. It is of great significance to achieve fast and accurate detection of targets. There are many application scenarios, such as automatic driving, face recognition, vehicle recognition, video surveillance, license plate recognition, mobile robots, and intelligent video surveillance systems. Target detection is also an important basis for advanced visual tasks such as behavior analysis and scene understanding, which will have a huge impact on subsequent target recognition. In addition, in real life, it is often necessary to detect multiple targets, and it is easy to have problems such as multitarget occlusion and self-rigid deformation. In recent years, with the development of information science and technology, coupled with the potential application of target detection, its practical value is extremely high and puts higher requirements on the accuracy of detection. Therefore, there is a need for a fast target detection algorithm with higher detection accuracy and better algorithm performance. Under the background of this era, the research on new has become the latest research hotspot. However, the research on target detection pays more attention to recognition efficiency, and there are not many fast detection methods, so it is necessary to choose the topic of this paper.

Regarding the field of target detection, in the early stages of computer vision development, when people search for specific targets in an image, they are usually implemented using simple and intuitive features and manually set rules. In 1990, the literature [1] proposed a method of template matching between simple geometric features such as arcs and corners and face templates for detecting faces. In 1995, the literature [2] proposed a method for detecting similar faces using a method of fuzzy matching between skin color distribution and facial texture features and face models. In 2004, Viola et al. proposed a classic face detection method [3], using the AdaBoost classification algorithm and Haar-like features and using the weak classifier cascade method, which is higher at the time of comparison. Accuracy and recall are also achieved in real time. In 2009, Dollár et al. proposed an integral channel feature [4], which included features of different channels such as color space, gradient, and amplitude gradient direction, using the AdaBoost classifier to filter the appropriate features in the feature pool of this feature. In 2010, a method of feature pyramid was proposed in the literature [5] to accelerate feature extraction. In 2014, Dollár combined the ideas of [4, 5]. In [6], an aggregate channel feature was proposed, using AdaBoost to select features, and a balance was found between accuracy and speed. In 2010, Pedro Felzenszwalb proposed a very successful target detection algorithm DPM (Deformable Part Model), which won the VOC 07, 08, and 2009 championships and became an important part of many image applications at that time. The algorithm takes into account multiple parts of the target for detection and has achieved good results in robustness, but its detection speed is about one or two frames per second, which is really unacceptable. In 2012, Krizhevsky et al. trained a large deep convolutional neural network AlexNet [7] in the ImageNet competition, classifying the 1.2 million images in the ImageNet competition into 1000 different categories, and the results are much better than the top algorithms. In 2014, Girshick et al. proposed the R-CNN deep convolutional [8], which is used in the field of target detection and has become a pioneering tool for deep learning as a target detection. It has exceeded the previous algorithm on the VOC 2012 dataset. The average accuracy rate of 30% has been compromised from this target detection field. In 2015, following R-CNN, Girshick personally improved the network and got the Fast R-CNN network [9]. Ren et al. made further improvements based on Fast R-CNN and proposed the Faster R-CNN [10] network. The author used an RPN network to extract candidate regions, replacing the previous selective search method, enabling end-to-end training. This not only speeds up the detection but also improves the accuracy of the detection. Target-specific detection for specific areas, such as face detection, has also developed unique methods to accelerate and improve accuracy. In 2015, Li et al. proposed a face detection method that combines AdaBoost and CNN and uses CNN to extract features and cascaded AdaBoost classifiers for classification [11]. In 2016, based on Li et al. [12], the face detection and face feature point location tasks were combined, and the multitask face detection and feature point regression network MTCNN was formed along with FDDB [13]. The dataset has one of the best levels of detection available and a near real-time detection speed on a single core CPU. It can be found that their research focuses on the efficiency of target detection, especially on the improvement of algorithm and the accuracy of recognition, but there is not much research on some broader targets.

In the research of target detection, for traditional target detection methods, target detection is generally divided into three stages. In the first stage, a sliding window frame is used to select candidate regions at different positions of a given image by using sliding window frames of different sizes. In the second stage, feature extraction is performed in these candidate regions; in the third phase, the classifier is used for identification. For different categories of objects, it is necessary to design corresponding different features and classification methods. For example, using the classic Harr [14] feature and Adaboosting [15] classifier, the sliding window search strategy is used for face detection; the features extracted by the Histogram of Gradients (HOG) [16] are subjected to support vector machine (SVM) [17, 18] for pedestrian detection; for general object detection, HOG features plus Deformable Part Model (DPM) [19] algorithm. In particular, the DPM algorithm has consistently won the VOC (Visual Object Class) 2007-2009 test champion in the traditional target test. In 2010, its author Felzenszwalb Pedro was awarded the "Lifetime Achievement Award" by the VOC. However, these algorithms need to manually obtain the relevant target feature information from the original input, and there are also many shortcomings. (1) Poor portability: for a specific inspection task, it is necessary to manually design different methods, and even for different targets or different shape states of the same target, the designer is required to have a higher level of experience. (2) Feature extraction and classification: training separation is a common problem of traditional detection models. If the extraction of artificial features occurs during the design process, the missing useful information will not be recovered from the classification training, thus affecting the detection results. (3) The traditional method uses the sliding window to perform traversal search and divides the picture into small pieces of various scales and sizes as much as possible and then recognizes the small pieces of the picture. Then, the small pieces of the picture are identified, the part with high probability is reserved, and the part with less probability is combined and deleted. The algorithm of this method is highly complex, and there are a large number of redundant small blocks, which undoubtedly seriously affect the running speed; even in reality, it is difficult to achieve through actual engineering.

In this paper, when studying the fast target detection algorithm, it is based on CFAR and target variance characteristics. First, regarding the CFAR (constant false alarm rate) algorithm, it has been used in a large amount. In the detection of high-resolution images of large scenes, algorithm in the field of SAR image is used. CFAR detection technology is a relatively common and effective detection method for radar target detection process. It enables the detector to adaptively detect radar targets in different clutter background environments. At the same time, the detector has a constant false alarm probability in different detection backgrounds.

The constant false alarm rate detection method was first applied to SAR image ship target detection, and it is the most commonly used and most effective type of detection algorithm [20–22]. From the statistical point of view, it can perform target detection with a certain false alarm probability, so it is widely used. Since the method uses the statistical distribution of the target and the background for analysis, it is also applicable to the visible light remote sensing image and is robust to the illuminance unevenness problem of the visible light image [23]. It is one of the most widely used methods because of its simple calculation, strong adaptability, and strong local statistical features. Since the 1960s, a lot of research has been done on the technique of constant false alarm rate, and many achievements have been made. Therefore, these algorithms have difficult bottlenecks in practical applications. With the continuous efforts of researchers, in 2007, researchers at the Institute for Infocomm Research proposed. These algorithms have low complexity and no prior information and are not subject to noise uncertainty. The advantages of influence have good application value. In addition, the Haar feature is also called the rectangular. It consists of simpler rectangles that form the template of the desired feature. The feature is first applied to the face representation, which is sensitive to some simple structures such as edges and line segments. Viola proposes to use the integral graph to calculate the value of the feature. After introducing the integral graph, each eigenvalue is calculated at a fixed time. Only one traversal calculation is needed for the image, which reduces the time for calculating the eigenvalue. Since the image has strong speckle noise, in order to detect a target with low contrast, the false alarm rate PFA should not be too small. The speckle noise will lead to a higher false alarm rate of the detection result, which increases the calculation amount of subsequent work. In the detection algorithm, the introduction of the variance feature can further reduce the false alarm. Therefore, the combination of CFAR and target variance characteristics can be applied to the research of fast target detection algorithms and can improve the performance and quality of fast target detection algorithms to some extent.

The background is complex and the noise interference is large, which makes it difficult to discriminate the real target. Therefore, suppressing noise and improving the contrast between the target and the clutter are helpful for improving the detection rate of the target. For low target detection efficiency and high false alarm rate of SAR image, this paper proposes a CFAR fast detection algorithm based on Rayleigh distribution and Gaussian distribution. The CFAR detection is divided into horizontal and vertical CFAR detection in two steps. The efficiency of parameter estimation is improved by the coincidence of adjacent point reference windows and the distribution characteristics of images. The algorithm combines the target variance characteristics to reduce the false alarm rate of the image. This paper conducts experiments on the MSTAR dataset to test the SAR images of self-propelled howitzers, armored reconnaissance vehicles, tanks, bulldozers, etc. The number of false alarms and the detection probability in different environments caused by artificial buildings in rural and suburban areas are compared. After prescreening, observe the relationship between the proportion of potential target pixels and the average running time of the total number of pixels in the SAR image, and visually display it in a line graph. Improve the proposed method compared existing detection algorithms; different CFAR detection algorithms are compared with the proposed method through experiments. The experimental results show that the proposed method can not only improve the image target detection effect but also effectively improve the target detection efficiency. It shows that the proposed fast target detection algorithm based on CFAR and target variance features has better performance.

## 2. Introduction

*2.1. Constant False Alarm (CFAR) Detection Method.* CFAR detection algorithm compares the gray value of each pixel in the SAR image with the adaptive detection threshold so that the target pixel is filtered out. The statistical distribution of the clutter around the target and the preset false alarm probability determine the size of the adaptive threshold. After the clutter statistical model is determined, the target is detected while ensuring that the preset warning probability remains the same, that is, given the false alarm rate. The key to the CFAR detection algorithm is to calculate the adaptive decision threshold (detection threshold) based on the preset false alarm probability. In other words, it is the key to CFAR detection. Common CFAR-based detectors are as follows. In this paper, we will compare the performance of CFAR operator based on Rayleigh distribution and CFAR detection based on Gaussian distribution.

*2.1.1. CFAR Operator Based on Rayleigh Distribution.* For the Rayleigh distribution, a good model can be established in the homogeneous region, but there is considerable error in fitting the heterogeneous region to the extremely heterogeneous region. The homogeneous region is capable of good model building, but there is considerable error in fitting heterogeneous regions to extremely heterogeneous regions. Compared with other models, Rayleigh distribution is an image model widely used in practical systems because its parameter estimation is simple and easy to implement. Many scholars have shown that CFAR can obtain better detection performance even if the assumed model does not describe the actual data distribution well. If the SAR clutter image obeys a simple Rayleigh distribution, then

$$f(x) = \frac{x}{b^2_s} e^{-x^2/2b_s^2}, \quad x > 0, \tag{1}$$

where $b_s$ is the shape parameter, and the mean $\mu_x$ and the variance $\sigma_x$ are

$$\mu_x = \sqrt{\frac{\pi}{2}} b_s = k_1 b_s \sigma_x = \sqrt{2 - \frac{\pi}{2} b_s} = k_2 b_s. \tag{2}$$

Regarding each pixel point $x_c$, a certain range area around the pixel point is taken as $a$, and then, a threshold value $x_0$ is determined $P_{\mathrm{FA}}$:

$$\begin{cases} \text{if } x_c > x_0, & \text{then } x_c \text{ is the target pixel,} \\ \text{else,} & x_c \text{ is a clutter pixel.} \end{cases} \quad (3)$$

The false alarm rate when the threshold is $x_0$ is

$$P_{\mathrm{FA}} = \int_{x_0}^{\infty} f_X\left(\frac{X}{\text{Clutter}}\right) dX. \quad (4)$$

Substituting $f(x)$ obeying the simple Rayleigh distribution into the above equation yields

$$P_{\mathrm{FA}} = \exp\left(-\frac{{x_0}^2}{2{b_s}^2}\right). \quad (5)$$

From the above false alarm rate calculation formula, we can see that the $P_{\mathrm{FA}}$ value is related to $x_0$ and $b_s$. In CFAR technology, scholars often use the mean and variance to calculate the threshold. Assume that

$$x_0 = \tau k_2 b_s + k_1 b_s = \tau\sigma_s + \mu_s, \quad (6)$$

where $k_1$ and $k_2$ are constants, $\tau$ is the alarm rate $P_{\mathrm{FA}}$, and $x_0$ is substituted into the expression of $P_{\mathrm{FA}}$ to obtain

$$P_{\mathrm{FA}} = \exp\left(-\frac{(\tau k_2 + k_1)^2}{2}\right). \quad (7)$$

Given the false alarm rate $P_{\mathrm{FA}}$, the corresponding $\tau$ size can be calculated according to the above formula. Therefore, we can continue to derive the expression of CFAR as follows:

$$\begin{cases} \text{if } \dfrac{x_c - \mu_s}{\sigma_s} > \tau, & \text{then } x_c \text{ is the target pixel,} \\ \text{else,} & x_c \text{ is a clutter pixel.} \end{cases} \quad (8)$$

*2.1.2. CFAR Detection Based on Gaussian Distribution.* Statistical theory is a mathematical theory that uses the statistical characteristics of signal and noise to establish the best decision. It mainly solves the problem of judging whether the signal exists or not in the observation disturbed by noise. Its mathematical basis is statistical judgment theory, also known as hypothesis testing theory. Hypothesis test is an important tool for statistical judgment, and signal detection is equivalent to hypothesis test in mathematical statistics. Hypothesis is the possible situation or state of the test object. For radar or sonar detection, two hypotheses can be selected, that is, whether the target exists or not. The two-parameter CFAR detection method based on Gaussian distribution is the most commonly used detection processing technology in the SAS field. Assuming that the clutter background obeys the

$$f(x) = \frac{1}{\sqrt{2\pi}} \exp\left(-\frac{(x-\mu)^2}{2\sigma^2}\right), \quad (9)$$

where $\mu$ is the average of the clutter; $\sigma$ is the standard deviation of the clutter, and its distribution function is expressed as

$$F(x) = \int_{-\infty}^{x} f(t)dt = \int_{-\infty}^{x} \frac{1}{\sqrt{2\pi}\sigma} e^{-(t-\mu)^2/2\sigma^2} dt. \quad (10)$$

Let $z = (t-\mu)/\sigma$ be substituted into the above formula to get the integral expression of the standard normal distribution:

$$F(x) = \int_{-\infty}^{(x-\mu)/\sigma} \frac{1}{\sqrt{2\pi}} e^{-z^2/2} dz = \Phi\left(\frac{x-\mu}{\sigma}\right). \quad (11)$$

Let the detection threshold be $T$, and if the false alarm probability is $P_{\mathrm{fa}}$, then

$$P_{\mathrm{fa}} = \int_{T}^{\infty} f(x)dx = 1 - F(T) = 1 - \Phi\left(\frac{T-\mu}{\sigma}\right). \quad (12)$$

By the above formula, the expression of the detection threshold is

$$T = \sigma\Phi^{-1}\left(1 - P_{fa}\right) + \mu. \quad (13)$$

In summary, when the clutter model is a Gaussian distribution, the detected threshold can be obtained according to the above formula. The two-parameter CFAR clutter models are therefore widely used. The above CFAR operator expression based on Rayleigh distribution is actually the same as the expression of the two-parameter CFAR based on Gaussian distribution in this section.

*2.1.3. CFAR Fast Algorithm.* The CFAR algorithm first assumes that the clutter data obeys a certain. The target of interest appears to be an extended target, and in most cases, multiple targets appear in the same scene. Therefore, in order to eliminate the influence of the target pixel on the parameter estimation of the clutter model, experts and scholars pay more attention to setting up a hollow sliding window with a protected area according to the size of the target so that they can start from the hollow sliding window, and they propose a large number of constant false alarm detection algorithm. Even if a clutter statistical model with high fitting accuracy has been obtained, the CFAR detection algorithm will encounter such a problem: when the sliding window moves on a SAR image, the clutter entering the annular area of the sliding window does not have to be uniform, and in many cases is uneven. The CFAR detector determines the sequence of clutter pixels for parameter estimation within the sliding window. In order to improve the detection speed of the target, the following method is used to reduce the amount of calculation. Think of the rectangular ring window as two parts: a horizontal window consisting of upper and lower borders and a vertical window consisting. It is clearly seen that most of the horizontal windows of adjacent pixels in the horizontal direction are coincident, and the upper and lower frames are different only by two pixels; the vertical direction is also similar. In this kind of coincidence, consider dividing the two-parameter CFAR into two steps: horizontal CFAR and vertical CFAR.

When estimating the mean, the horizontal CFAR processes the image line by line, and the reference window of each pixel is the pixel in the upper and lower borders. Calculate the mean of the reference window for the first pixel of each row. Then, consider the remaining pixel points of the row, and when calculating, it is only necessary to appropriately correct the previous adjacent pixel. Vertical CFAR is similar to horizontal CFAR. After using the above method, the calculation amount of the mean estimation is greatly reduced. Taking a $1780 \times 1470$ image as an example, if the length of the reference window is set to 95, it is estimated that the addition of the background mean is reduced by more than 90%.

Since the calculated amount of the estimated mean is much smaller than the calculated amount of the estimated background variance, further improve the efficiency of the algorithm; the following method is used to reduce the number of variance estimates. The variance to mean ratio (DMR) of the Rayleigh distribution is a constant $t$:

$$\mathrm{t} = \frac{\sigma_s}{\mu_s} = \sqrt{\frac{4-\pi}{\pi}} = 0.5227. \tag{14}$$

Through the experiment of a large number of clutter images, in the distribution of the ratio of variance to mean, most of the DMR values are distributed around 0.6, and all DMR values are above 0.51. Taking $t = 0.5$, then perform the first CFAR test with the CFAR operator expression based on the Rayleigh distribution. If the point is determined to be a clutter pixel, the next point is processed; otherwise, estimate the variance of the reference window and then perform the second CFAR test. When performing target detection, most of the pixels are judged as clutter pixels in the first CFAR test, so only the variance of the minority reference window needs to be calculated. Experiments on $5\,\mathrm{km}^2$ SAR images show that the estimated number of background variances is reduced by more than 80% on average using the clutter distribution characteristics.

*2.2. Target Variance Characteristics.* In order to detect the target with low contrast, the false alarm rate $P_{\mathrm{FA}}$ value should not be set too small, resulting in a higher false alarm of the detection result. Experiments show that in SAR images, the variance of natural clutter is significantly smaller than the variance of the target region. We can take advantage of this remarkable feature of the target to reduce false alarms. When performing horizontal and vertical CFAR detection, the variance $\sigma_c$ of a smaller neighborhood $N_c$ (including the point) is further calculated for each pixel that is determined to be the target. Only when $\sigma_c$ is greater than a certain multiple variance is the point as the target pixel. That is

Figure 1: Four types of optical images.

$$\begin{cases} \text{if } \sigma_c > M_1\sigma_s, & \text{then } x_c \text{ is the target pixel,} \\ \text{else,} & x_c \text{ is a clutter pixel,} \end{cases} \tag{15}$$

where $M_1$ is a constant determined experimentally.

In the CFAR detection, the false alarm can be significantly reduced by adding the local variance feature.

*2.3. Rapid Prescreening Method.* According to the histogram adaptive adaptation of the SAR image, the global preselected global threshold $T_{\mathrm{g}}$ is determined. $A$ is assumed to be the amplitude value of the corresponding pixel. After the prescreening, the proportion of the potential target of the entire SAR image is $P_{\mathrm{t}}$. The threshold $T_{\mathrm{g}}$ can be determined: $P(A > T_{\mathrm{g}}) = P_{\mathrm{t}}$.

$P$ is the probability value; $P_{\mathrm{t}}$ is the empirical value, and the variation range is between 0 and 1. In general, in large SAR images, the value of $P_{\mathrm{t}}$ is relatively small. Then, when the pixel value of the image point to be detected $(i, j)$ is greater than $T_{\mathrm{g}}$, the point is a potential target point, and further fine detection is required; otherwise, the point is determined to be a clutter pixel, which can be directly filtered out.

*2.4. Location of the Area of Interest.* In the results of the CFAR detection, there are many isolated bright spots. Before locating the region of interest (ROI), consider using a majority filter to filter it. A pixel that is simultaneously targeted by horizontal CFAR and vertical CFAR is more likely to be a target, and this information is retained by the summation result of the CFAR detection. In most filters, the weight of a pixel that is simultaneously determined by two CFARs is $M_3$ times the weight of a pixel that is only determined by one CFAR. $M_3 > 1$, the specific value of which is determined by experiment. In the integrated CFAR test results, the target pixel is generally a bright spot, and the background false alarm is generally gray. After passing through a majority of filters with weights, the target area will be further enhanced and its false alarm highlights will be significantly reduced. The filtered image is a binary image. The bright dots represent the target and the dark dots represent the background. Check each connected area. If its area (that is, the number of pixels) is in the range $[A1, A2]$, then this is the potential target area, that is, the area of interest.

## 3. Experiments

*3.1. Data Sources.* This data is mostly a SAR slice image of a stationary vehicle on the ground, which contains the target

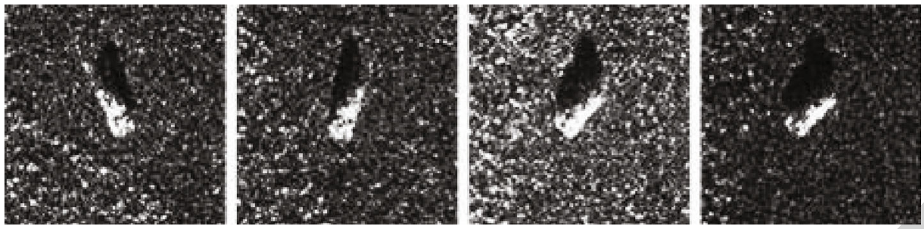

Figure 2: SAR image.

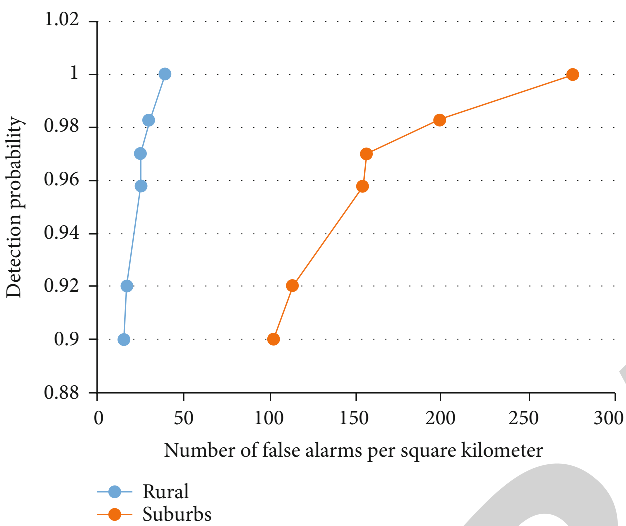


Figure 3: Detection performance in different environments (rural, suburban).

images obtained by various vehicle targets at various azimuth angles. The training target image data obtained at 17 degrees of the radar working pitch angle include three categories: T72 (tank), BMP2 (step chariot), and BTR70 (armored transport vehicle); the test set is the radar working pitch angle which is the target image data obtained at the time; the dataset also contains three categories, T72 (tank), BMP2 (step chariot), and BTR70 (armored transport vehicle). In these datasets, these targets are images of the various targets in the direction of the radar when the radar is operating at a variety of different elevation angles. Different types of targets also include different models. The same type of target but different models has some differences in their equipment, but their overall scattering characteristics are similar.

*3.2. Experimental Evaluation Criteria.* In the field of target detection: accuracy and recall.

Check the correct situation: TP (true positive): the object is originally a positive example, and the network recognition is a positive example.

TN (true negative): the object is originally a negative example, and the network is identified as a negative example.

Detecting an error: FP (false positive): the object is originally a negative example, and the network identification is a positive example, usually called false positive.

FN (false negative): originally a positive example, the network is identified as a negative example, usually called underreporting.

In the target detection task, the positive example is usually the object that is desired to be detected in the experimental image, and the negative example is usually expressed as a background other than the positive exception. Accurately describe the detection, the calculation method of accuracy and recall (recall) is as follows:

$$
\begin{aligned}
P &= \frac{\mathrm{TP}}{\mathrm{TP}+\mathrm{FP}}, \\
R &= \frac{\mathrm{TP}}{\mathrm{TP}+\mathrm{FN}}.
\end{aligned} \tag{16}
$$

In the formula, $P$ refers to the precision, correct positive case in all the positive examples identified. $R$ refers to the recall, which represents the proportion of the correct positive case in all true positive examples of the sample.

*3.3. System Environment.* The research is of fast target detection algorithm based on CFAR and target variance feature.

## 4. Results and Discussions

*4.1. Result 1: SAR Image and Test Result.* The four types of optical images of the ground targets in the MSTAR dataset are shown in Figure 1. From left to right, they are self-propelled howitzers, armored reconnaissance vehicles, tanks, and bulldozers. The SAR image is tested by the combination of CFAR and target variance features. The SAR image is shown in Figure 2. In the figure, bright dots represent pixel points that are simultaneously judged as targets in horizontal CFAR and vertical CFAR detection, and dark dots represent pixel points that are judged to be clutter in both detections, and the gray dots in between indicate the pixel points that are judged as targets in the CFAR detection in only one direction. It can be seen that most of the target pixel points are detected in the CFAR detection in both directions, and the false alarm around the vehicle is generally detected only by the detector in one direction. The test results corresponding to the war cars parked alone are brighter, while the results of some buildings in the horizontal or vertical direction are mostly gray.

*4.2. Result 2: Number of False Alarms and Detection Probability in Different Environments.* The clutter images are divided into suburban and rural categories, each with

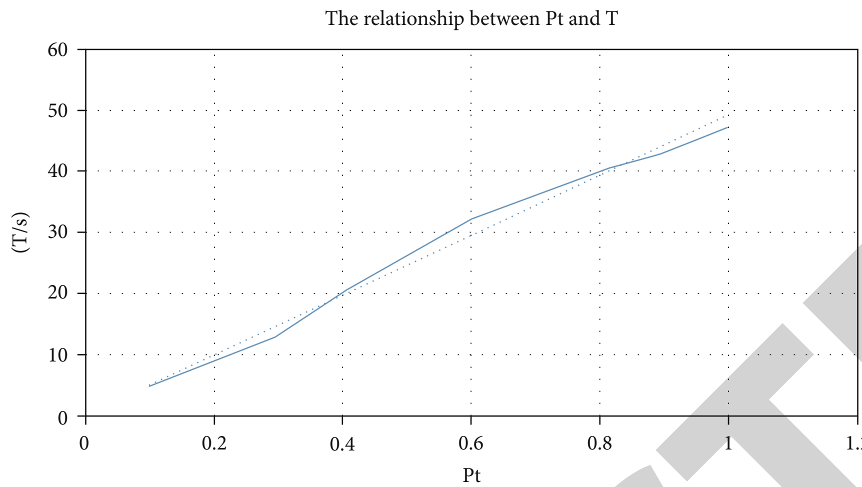


Figure 4: Relationship between the proportional value $P_t$ and the average running time $T$.

Table 1: Comparison of performance of different CFAR detection algorithms.

| | Number of real targets | Number of detection targets | Number of false alarm targets | Operation time (s) |
|---|---|---|---|---|
| CA-CFAR | 22 | 21 | 2 | 157.2 |
| GO-CFAR | 22 | 20 | 3 | 78.4 |
| SO-CFAR | 22 | 21 | 2 | 31.25 |
| Method of this paper | 22 | 22 | 1 | 16.1 |

Table 2: The comparison of several typical SAR image target detection algorithms.

| Number | Super pixel | CFAR | AdaBoost |
|---|---|---|---|
| 1 | Higher | Generally | Higher |
| 2 | Like | Generally | Poor |
| 3 | Lower | Higher | Like |

Table 3: Some performance parameters of the GTX 1080 Ti graphics card used in the experiment.

| | |
|---|---|
| Video memory | 11264 MBytes |
| Shared memory/block | 49152 bytes |
| Bandwidth | 352-bit |
| Maximum clock frequency | 1633 MHz |
| Constant memory | 65536 bytes |
| Maximum number of threads/block | 1024 |
| Warp size | 32 |

45 and 5 images. There are many buildings in the suburban image, while the ground objects in rural images are mainly independent trees, grasslands, woods, lakes, etc. The sizes of the images used in the experiments are not the same, but most of the images are about $1780 \times 1470$, which represents a floor area of about $0.1\,\text{km}^2$. The target data contains images of three targets. Each of the three types of images has about 200 images, and each target image has a size of $128 \times 128$. After detecting the target image and the clutter image, the detection probability and the false alarm in different environments are obtained. The result is shown in Figure 3. The higher the detection rate of the target, the more false alarms there are. In practical engineering applications, appropriate choices should be made for detection probabilities and false alarms based on actual needs. With relatively large number of artificial buildings in the suburbs, the number of false alarms in suburban images is significantly higher than that in rural areas.

*4.3. Result 3: Quick Prescreening.* Using the classical Gaussian distribution function-based two-parameter CFAR detection, when the false alarm probability is $1.0 \times 10 - 5$, set $P_t$ to 0.1~1, and perform 100 simulations for each value to obtain corresponding $P_t$. The average running time under the value is $T$, as shown in Figure 4. That as $P_t$ decreases, the operation time is substantially linearly decreasing with $P_t$, and the decreasing multiple is basically the same as the reciprocal of $P_t$.

In practical applications, the $P_t$ value should be set reasonably according to the proportion of the target point in the whole SAR scene. When the $P_t$ value is too large, the efficiency of the fast algorithm is limited, performance; if the $P_t$ value is too small, it may cause the false alarm to be missed, resulting in the loss of the target that really needs to be detected. It should be pointed out that the results of rapid prescreening have the characteristics of irreversibility in the later processing. That is to say, if a target pixel is determined to be a clutter pixel in the fast prescreening process,

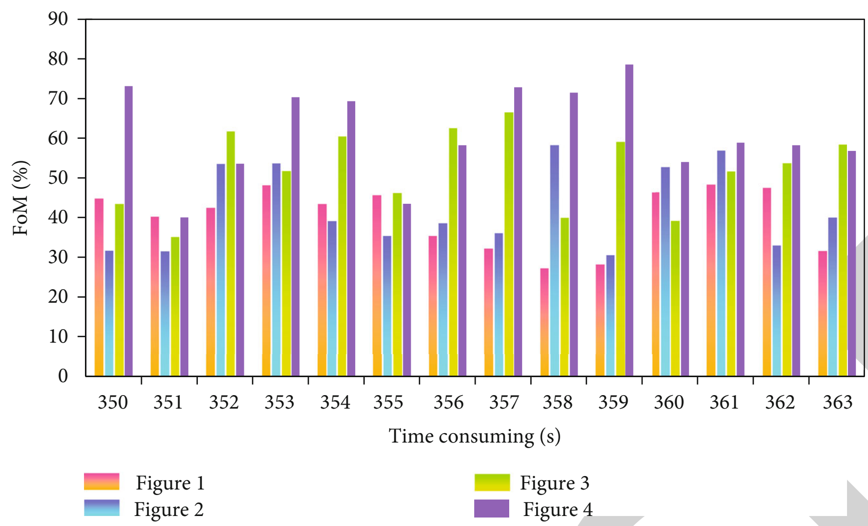


Figure 5: The experimental results.



subsequent detection will generally not change the category of the pixel again.

*4.4. Result 4: Performance Comparison of Different CFAR Detection Algorithms.* The experiment studied based on CFAR detection such as CA-CFAR, GO-CFAR, and SO-CFAR. In the case where the number of real targets is the same, after using the detection algorithm, the detection number of targets and the running time required for the algorithm to complete the detection process are recorded, and the results are shown in Table 1.

According to Table 1, the method has the largest. Moreover, false alarm targets in this method are small, which indicates that in the CFAR detection, the false alarm can be reduced by adding the local variance used in this paper which is much shorter than other CFCA methods when performing target detection. It has the advantages of high detection rate, less false alarm, and faster speed.

SAR image target detection refers to the detection of objects of interest in SAR images, and the bounding boxes are used to demarcate them in the SAR images to serve the subsequent identification and classification stages. The comparison of several typical SAR image target detection algorithms is shown in Table 2.

Some performance parameters of the GTX 1080 Ti graphics card used in the experiment are shown in Table 3.

To illustrate the role of convolutional layers, the following experiments were performed. Remove the convolution layer in the CP-CFAR algorithm and use GPU to perform target detection in parallel, and compare the detection time. The experimental results are shown in Figure 5. For four different images, the performance of algorithm labels is different. Generally speaking, the FOM value of image 4 is the highest, and that of image 2 is the lowest.

## 5. Conclusions

In view of the current situation of the target method in the field of target performance and the lack of accuracy, this paper focuses on the CFAR and target variance characteristics. In this paper, a fast Rayleigh and Gaussian is proposed. The CFAR detection is divided into two steps: horizontal and vertical CFAR detection. The efficiency of parameter estimation is improved by the coincidence of adjacent point reference windows and the distribution characteristics of images. The algorithm in this paper combines the target variance characteristics to reduce the false alarm rate. The experiment was performed on the MSTAR dataset. The algorithm in this paper combines the target variance characteristics. The experiment was performed on the MSTAR. The experimental results verify the proposed method. The fast and target variance feature proposed in this paper has the characteristics of high detection rate, less false alarm, and fast speed, and its detection performance is good. In practical applications, the detection algorithm can automatically adjust system parameters according to the requirements of detection probability and false alarm probability to adapt to different image and target requirements. The fast conditions and basis for further application in SAR image target detection contribute to the development and application of ATR technology in SAR images. Therefore, the combination of CFAR and target variance characteristics can be applied to the research of fast target detection algorithms and can improve the performance and quality of fast target detection algorithms to some extent.

## Data Availability

No data were used to support this study.

## Conflicts of Interest

The authors declare that the research was conducted in the absence of any commercial or financial relationships that could be construed as a potential conflict of interest.

## Acknowledgments

This work was supported by the Key Research and Development Plan Guidance Project of Cangzhou (204102014).

## References


[1] V. Govindaraju, S. N. Srihari, and D. B. Sher, "A computational model for face location," in *Proceedings Third International Conference on Computer Vision*, pp. 718–721, Osaka, Japan, 1990.

[2] Q. Chen, H. Wu, and M. Yachida, "Face detection by fuzzy pattern matching," in *Proceedings of IEEE International Conference on Computer Vision*, Cambridge, MA, USA, 1995.

[3] P. Viola and M. J. Jones, "Robust real-time face detection," *International Journal of Computer Vision*, vol. 57, no. 2, pp. 137–154, 2004.

[4] P. Dollar, Z. Tu, P. Perona, and S. Belongie, "Integral channel features," in *Procedings of the British Machine Vision Conference 2009*, London, UK, 2009.

[5] P. Dollár, S. Belongie, and P. Perona, "The fastest pedestrian detector in the west," in *British Machine Vision Conference*, pp. 1–11, Aberystwyth, UK, 2010.

[6] P. Dollar, R. Appel, S. Belongie, and P. Perona, "Fast feature pyramids for object detection," *IEEE Transactions on Pattern Analysis & Machine Intelligence*, vol. 36, no. 8, pp. 1532–1545, 2014.

[7] A. Krizhevsky, I. Sutskever, and G. E. Hinton, "ImageNet classification with deep convolutional neural networks," *Advances in Neural Information Processing Systems*, vol. 25, no. 2, 2012.

[8] R. Girshick, J. Donahue, T. Darrell, and J. Malik, "Rich feature hierarchies for accurate object detection and semantic segmentation," in *Proceedings of the IEEE conference on computer vision and pattern recognition*, pp. 580–587, Columbus, OH, USA, 2013.

[9] R. Girshick, "Fast R-CNN," in *Proceedings of the IEEE international conference on computer vision*, pp. 1440–1448, Santiago, Chile, 2015.

[10] S. Ren, K. He, R. Girshick, and J. Sun, "Faster R-CNN: towards real-time object detection with region proposal networks," *Advances in Neural Information Processing Systems*, vol. 28, 2015.

[11] H. Li, Z. Lin, X. Shen, J. Brandt, and G. Hua, "A convolutional neural network cascade for face detection," in *Proceedings of the IEEE conference on computer vision and pattern recognition*, pp. 5325–5334, Boston, 2015.

[12] K. Zhang, Z. Zhang, Z. Li, and Y. Qiao, "Joint face detection and alignment using multitask cascaded convolutional networks," *IEEE Signal Processing Letters*, vol. 23, no. 10, pp. 1499–1503, 2016.

[13] V. Jain and E. Learned-Miller, *FDDB: a benchmark for face detection in unconstrained settings*, UMass Amherst Technical Report, 2010.

[14] R. Lienhart and J. Maydt, "An extended set of Haar-like features for rapid object detection," in *Proceedings. international conference on image processing*, pp. 900–903, IEEE, Rochester, NY, USA, 2002.

[15] P. Viola and M. Jones, "Rapid object detection using a boosted cascade of simple features," in *Proceedings of the 2001 IEEE Computer Society Conference on Computer Vision and Pattern Recognition (CVPR2001)*, pp. 511–518, IEEE, Kauai, HI, USA, 2003.

[16] N. Dalal and B. Triggs, "Histograms of oriented gradients for human detection," in *IEEE Computer Society Conference on Computer Vision and Pattern Recognition (CVPR2005)*, pp. 886–893, IEEE, San Diego, CA, USA, 2005.

[17] V. Cortes, C. Cortes, and V. Vapnik, "Support-vector networks," *Machine Learning*, vol. 20, no. 3, pp. 273–297, 1995.

[18] L. Cf and W. Sd, "Fuzzy support vector machines," *IEEE Transactions on Neural Networks*, vol. 13, no. 2, pp. 464–471, 2002.

[19] D. Forsyth, "Object detection with discriminatively trained part-based models," *Computer*, vol. 47, no. 2, pp. 6-7, 2014.

[20] U. Srilakshmi, N. Veeraiah, Y. Alotaibi, S. Alghamdi, O. I. Khalaf, and B. V. Subbayamma, "An improved hybrid secure multipath routing protocol for MANET," *IEEE Access*, vol. 9, pp. 163043–163053, 2021.

[21] M. Rajalakshmi, V. Saravanan, V. Arunprasad, A. T. Romero, I. Khalaf, and C. Karthik, "Machine learning for modeling and control of industrial clarifier process," *Intelligent Automation & Soft Computing*, vol. 32, no. 1, pp. 339–359, 2022.

[22] O. I. Khalaf, G. M. Abdulsahib, and B. M. Sabbar, "Optimization of wireless sensor network coverage using the bee algorithm," *Journal of Information Science and Engineering*, vol. 36, no. 2, pp. 377–386, 2020.

[23] Z. Lv and H. Ko, "Introduction to the special issue on recent trends in medical data security for e-health applications," *ACM Transactions on Multimidia Computing Communications and Applications*, vol. 17, 2021.